TELKOMNIKA, Vol.16, No.6, December 2018, pp.2661~2667
ISSN: 1693-6930, accredited First Grade by Kemenristekdikti, Decree No: 21/E/KPT/2018
DOI: 10.12928/TELKOMNIKA.v16i6.9563

Thermodynamic Performance and Wave Propagation Sensor System of Fiber Bragg Grating in Liquid Media

Romi F. Syahputra[1], Ridho Kurniawan[2], Yunita I. Lubis[3], Mesra Sania[4], Okfalisa[5], Saktioto[6]*
[1,3,4,6]Department. of Physics, Faculty of Mathematics and Natural Sciences, Universitas Riau
HR. Soebrantas St. Km 12.5, Pekanbaru 28293, Indonesia, telp/fax: (0761) 63273
[2]Baristand Industri Banda Aceh
Cut Nyak Dhien St. No. 377, Lamteume Timur, Banda Aceh, Indonesia, telp/fax: (0651) 49714
[5]Information Technology Dept, Faculty of Science and Technology, UIN Suska
HR. Soebrantas St. Km 15, Pekanbaru 28293, Indonesia
*Corresponding author, e-mail: romifadlisyahputra@yahoo.com[1], ridho.kurniawan@student.unri.ac.id[2], irluubis25.yunita@gmail.com[2], saniania07@gmail.com[4], okfalisa@yahoo.com[5], saktioto@ieee.org[6]

Abstract

Although the measurement of liquids temperature is commonly used by Fiber Bragg Grating (FBG) sensor but its thermodynamic performance has interesting phenomena. This paper proposes the measurement and simulation of liquids temperature using FBG. Laser diode was launched into human blood, water, and vegetable oil, then transmitted power is measured by optical powermeter to determine its corresponding temperature. The results showed that the increasing temperature changes led to the widening of the wave shift. The largest change of wavelength is water temperature and the smallest One is vegetable oil temperature. Increase in liquid temperature causes the output power is greater. FBG simulation of sine and square function are also designed for temperature range of 30 °C to 41 °C with matrix transfer method based on coupled mode theory. Peak value of transmission spectrum of each function is shown by the change of temperature which indicates the sensor is sensitive to sine and square function variations. The peak at temperature of 30°C for each sine and square are -78.32 dB and -102.66 dB and increased to 41 °C at 46.72 dB and -79.89 dB, respectively.

Keywords*: fiber Bragg grating, liquids temperature, transmission spectrum*

1. Introduction

Temperature measurements play as an important role in many applications, especially in the medical and industrial fields. Thermocouples and thermistors have been widely used for temperature measurement in industrial and medical applications [1], but in their application have limitations due to high electromagnetic stress and interference. The development of optical fiber technology nowadays has grown rapidly and widely used in communication and delivery information system [2, 3]. Fiber optic sensors can be used as an alternative technology providing solutions in overcoming several conditions. FBG technology is one of the most popular choices for temperature measurement [1], having a function of filter or sensor, it also has a specific characteristic of Bragg wavelengths that can be affected by environmental changes such as temperature and strain. FBG-based sensors have been widely used in fluid temperature measurements such as tilted FBG types used for temperature measurement and refractive index of several types of liquids [4, 5]. Such systems have the ability for more sensitive measurements to external disturbances, such as changes in temperature, strain, deformation and pressure from a detectable material [6-12]. Although FBG has successfully detected the objects by physical magnitudes, in term of liquid media, the performance design of FBG still has interesting phenomena for the wavelength and filter when interacting to the liquids.

This paper investigates the FBG performance when measuring temperature of human blood fluid, water, and vegetable oil. It is immersed in liquid that has been removed from the coolant and launched an infrared laser diode source having a wavelength of 1550 nm with an input power of -5 dBm. Optical power changes when measuring liquids at optical power detectors. Liquid temperatures are calculated by shifting the Bragg wavelength due to power changes. FBG as a temperature sensor is also numerically designed to support experimental

Received April 10, 2018; Revised October 3, 2018; Accepted November 1, 2018

set up. We also developed FBG simulation to measure the blood temperature. Using a simulation method with a computer device then it produces the solution of the problem [13]. This research simulates the optical properties of grating shapes of sine and square in the temperature range 30-41 °C. The physical parameters of the grating determined based on Corning® SMF-28e+® products.

2. Methodology

The uniform FBG is experimentally designed along 10mm using a striper. This study begins by measuring the vegetable oil, the blood and water detected at the power output. The liquid will be frozen in the coolant before measuring the samples. They are performed by varying the temperature about 30 minutes of the blood, water, and vegetable oil. The schematic diagram of experiment set up is shown in Figure 1.

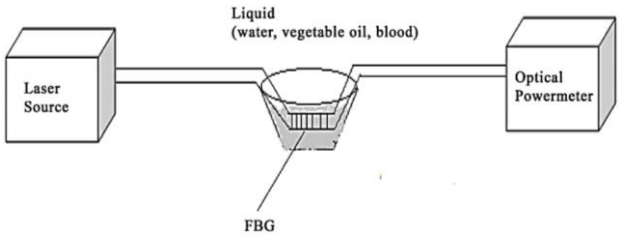

Figure 1. Experimental set up of optical FBG measurement

Experimentally, a diode laser source with an input power of -5 dBm and a wavelength of 1550 nm propagates to FBG. The influence of liquid temperature on FBG resulted in a shift of grating period and the refractive index via the thermal expansion coefficient. The shift of grating period and refractive index can cause the shift of Bragg wave peak. The non-reflected waves will continue to propagate to the output which are detected by the optical power. The reflected power will change if the Bragg wavelength changes. Rays passing through FBG dipped in the blood will experience a grating shift with the FBG system under normal circumstances. The temperature of the blood is calculated from the Bragg wavelength shift λ_B.

By simulation, the coupled mode theory with the matrix transfer equation can be expressed in following [14], namely:

$$T_i \begin{bmatrix} \cosh(\gamma l_i) - i\frac{\Delta\beta}{\gamma}\sinh(\gamma l_i) & -\frac{k}{\gamma}\sinh(\gamma l_i) \\ i\frac{k}{\gamma}\sinh(\gamma l_i) & \frac{k}{\gamma}\sinh(\gamma l_i) \end{bmatrix} \quad (1)$$

where κ represents coupling coefficient, and $\Delta\beta$ represents detuning wave vector by $\Delta\beta = \beta - \pi/\Delta$ and $\gamma = \sqrt{k^2 - \Delta\beta^2}$ then $\beta = 2\pi n_{eff}/\lambda$ [15]. The physical parameters are the core and cladding radii ari 4,1 μm and 62,5 μm, respectively, wavelength of 1550 nm and effective refractive indices for core and cladding ari 1,4674 and 1,4607, respectively. The grating parameters are given in Table 1. The fiber modes used are single mode fiber with variations of grating to temperature on sine and square shaped from 30-41 °C to produce the transmission and reflection spectrum function against the wavelength.

Table 1. Grating Parameter for Simulation

Parameter	Marks
Grating shape	sine and rectangle
Average index	uniform
Period chirp	no
Apodization	uniform
Grating length	5×104□m
Number of segments	25
Period	0,529μm

3. Result and Discussion

The output power at the detector and the reference temperature is investigated. There is a shift in Bragg wavelength due to the treatment with three liquids as shown in Figure 2. The change of Bragg wavelength in water is greater than that of vegetable oil, which are 0.3559-0.2209 nm shown by a grating shift in the wider Bragg grating fibers. Wide changes in Bragg wavelengths are followed by changes in water temperature that is from solid (ice) to melt at -5.10 °C to 4.42 °C. This indicates that water has a small viscosity, whereas changes in Bragg wavelengths in vegetable oil are smallest, i.e., 0.2169-0.1595 nm described by the shorter grid shifts in the Bragg gratingand the highest viscosity of vegetable oil followed by changes in the temperature of vegetable oil which is also smaller i.e., 4.71- 8.75 °C. The increment in the blood temperature causes a grating shift in the wide Bragg grid fibers as indicated between water and vegetable oil, i.e., 0.28 - 0.21 nm. It is not suprising when the water is faster response compared to others since the energy released from water (by increasing the temperature), more energy is absorbed by FBG readily rather than is held by the internal thermal energy as a binding molecules for water corresponding to smaller viscosity. On the other hand, FBG is slightly late to catch up energy respond for the blood even for vegetable oil with a highest viscosity, much thermal energy absorbed of both samples from circumferences (increment of temperatures) are kept to be stored as internal molecular binding energy, so that the change of wavelength Bragg is very small when temperature of samples increases.

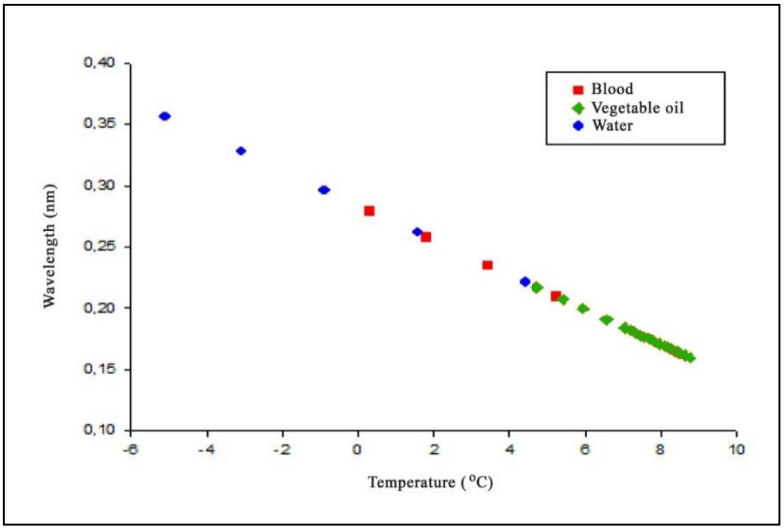

Figure 2. Bragg wavelengths response for various liquids

It detected from output power as depicted in Figure 3, the higher the liquid temperature increases the greater the output power will be by the widening of the Bragg grid. Although the energy is conservative and no power losses due to reflection and transmission of wavelength source, and frequency is maintained, the higher constant power explains that the intensity of power is launched readily since there is less resistance or absorption of FBG by sample viscosity changes. In contrast, the increment of temperature is to widen the Bragg grating but not to reduce the power itself. The highest power output in the range of -16.92 dBm to -16.905 dBm of the blood indicates that it has the greatest density and vice versa for vegetable oil. Where the vegetable oil will be allowed to absorb the energy from the wavelength source in the range of -38.93 dBm to -37.63 dBm. The power losses occurring in the optical circuit may affect the optical power.

Figure 4 shows that the temperature profile in human blood and water is relatively increases and fluctuates but not for vegetable oil. This is due to Bragg's grating shift response to temperature changes. Fluctuated oscillations in human blood and water temperature indicate mixed-liquid response of so that the FBG tend to response faster compared to temperature changes corresponding to the larger grating shift to adapt with cooling liquid. On the other hand,

no occurrence of fluctuations in vegetable oil temperatures is due to a shorter grating shift resulting in the absence of repetition of output power values.

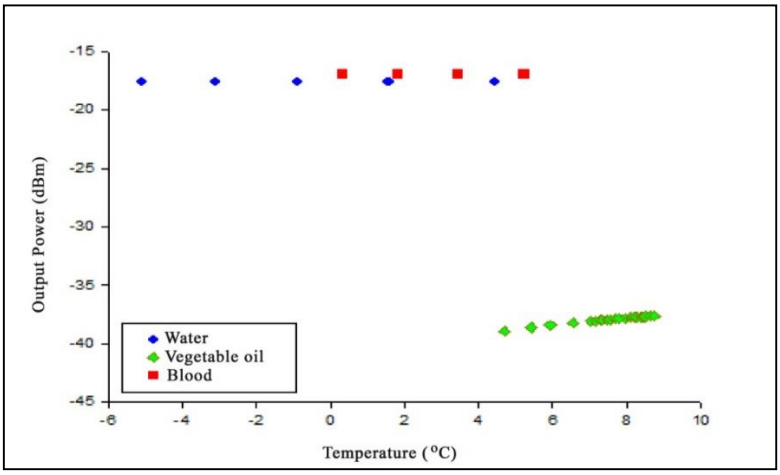

Figure 3. Output power and temperature for various liquids

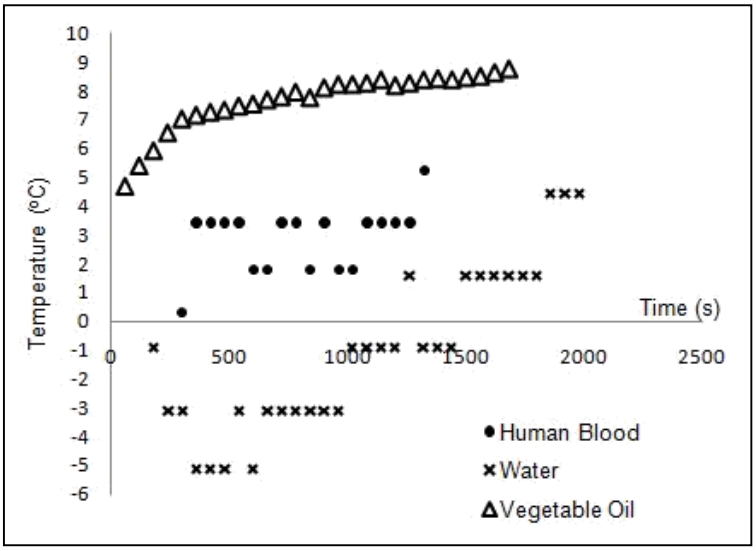

Figure 4. Temperature measured of the liquids by FBG

In simulation, the characteristics of the transmission spectrum generated from the FBG model through a single-mode fiber from 30 °C to 41 °C for every 1 °C with sine and square shape are described. The transmission comparison value for the square and sine grating shape is depicted in Figure 5. The sine-shaped grating has a greater transmission rather than the square-shaped. This dicrepancy is due to the faster sine shape allows the wavelength source to propagate to sinusoidal trajectory to the output edge of fiber so that the required input power of the sine grating form is much faster transmission. The condition of increasing the transmission to temperature causes the transmission spectrum to experience smaller power losses, so that the peaks of the transmission spectrum experience a shift in which the energy transmitted by the fiber will be greater. The rising temperatures cause the peak position of the transmission spectrum to shift. The result of simulation for sine-shaped of FBG at 30 °C and 41 °C is described in Figure 6 (a) and (b) respectively, which the transmission was increase from -78.32 dB at 30 °C to -46.72 dB at 41 °C.

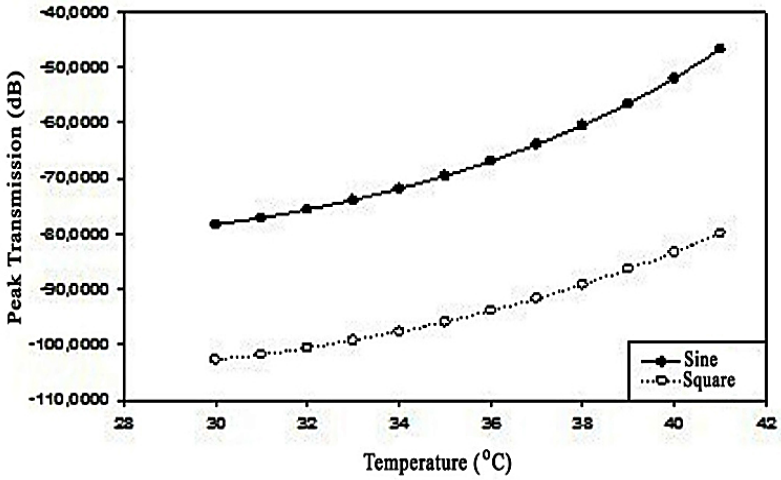

Figure 5. FBG sine and square shape peak for various temperatures

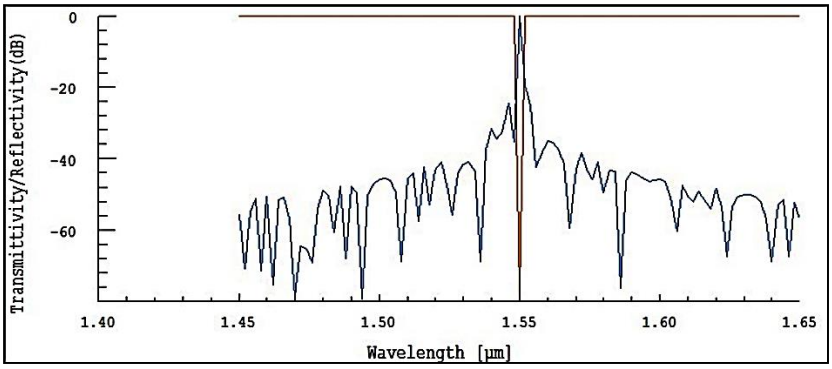

(a)

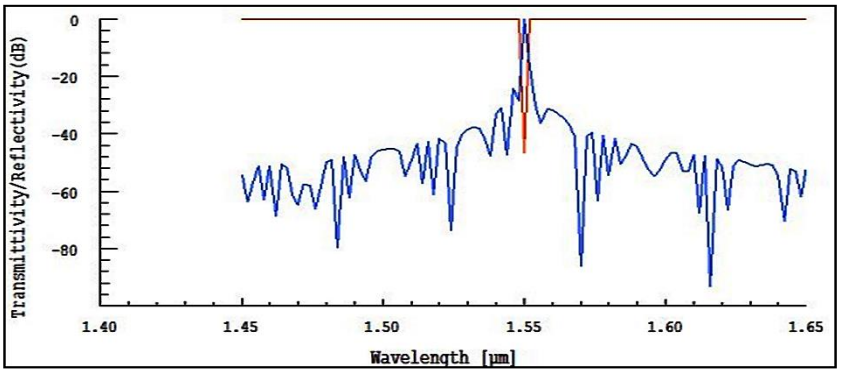

(b)

Figure 6. Transmission and reflection to the wavelength with the fiber shape of the sine grating at (a) 30 °C and (b) 41 °C.

The simulation results of FBG for square grating shape can be seen in Figure 7. In Figure 7, the spectral waves have two functions, transmission (red line) with a stright line and reflection (blue line) with a fluxtuated pattern. The temperature rise, from 30 °C to 41 °C, causes the peak value of the transmission spectrum to shift -102.66 dB to -79.89 dB, but it does not change the value of the transmitted wavelength of 1550 nm due to the filter of wave, however;

several reflection waves tend to occur as many as transmission waves but this disturbance can not affect the dominant transmission.

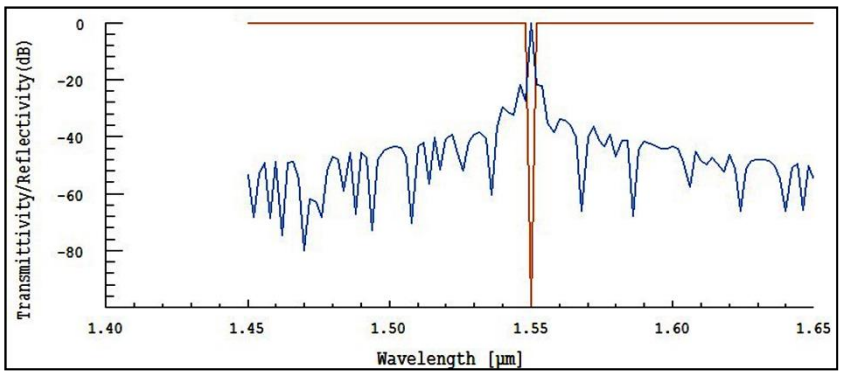

(a)

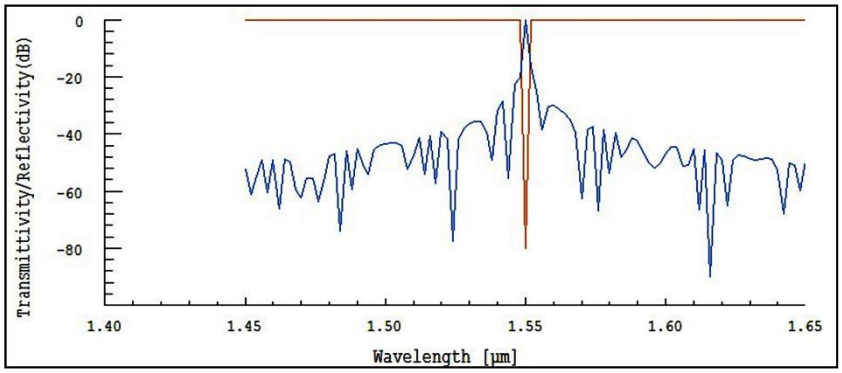

(b)

Figure 7. Transmission and reflection to the wavelength with the square grating fiber shape at (a) 30 °C and (b) 41 °C

4. Conclusion

FBG has successfully measured the temperature of water, human blood and vegetable oil showing the FBG wavelength is directly proportional to the temperature. The largest change in Bragg wavelengths is found in water temperature measurements, i.e., in the range 0.3559-0.2209 nm and the smallest one is vegetable oil temperature, in the range 0.2169-0.1595 nm. The increase of liquid temperature to the FBG causes the higher output optical value of the detector. The blood temperature measurement has the highest output power in the range of -16.92 dBm to -16.905 dBm and the lowest one is vegetable oil in the range of -38.93 dBm to -37.63 dBm.

The simulation results have also showed the temperature with the shifting peaks of the spectrum transmission. Two sine and square grating designs show the various transmission peaks of temperature which is respectively -78.32 dB and -102.66 dB for 30 °C and increases up to -46.72 dB and -79.89 dB for 41 °C. All temperature results are in a transmission wavelength of 1550 nm but other wavelength of reflections and transmissions vary greatly.

Acknowledgment

We would like to thank the University of Riau and Ministry of Research and Higher Education for generous and financial support of this research project in 2017.

References

[1] Hoffmann L, Müller MS, Krämer S, Giebel M, Schwotzer G, Wieduwilt T. *Applications of fibre optic temperature measurement*. Proceedings of the Estonian Academy of Sciences Engineering. 2007: 13(4): 363–378.

[2] Agrell E, Karlsson m, Chraplyvy AR, Richardson DJ, Krummrich PM, Winzer P,Roberts K, Fischer JK, Savory SJ, Eggleton BJ, Secondini M, Kschischang FR, Lord A, Prat J, Tomkos I, Bowers JE, Srinivasan S, Pearce MB, Gisin N. Roadmap of optical communications. *Journal of Optics*, 18 (6): 063002-1—063002-40. DOI: https://doi.org/10.1088/2040-8978/18/6/063002.

[3] Syahputra RF, Saktioto, Meri R, Syamsudhuha, Okfalisa. Profile of Single Mode Fiber Coupler Combining with Bragg Grating. *TELKOMNIKA Telecommunication Computing Electronics and Control*. 2017; 15(3): 1103-1107. DOI: http://dx.doi.org/10.12928/telkomnika.v15i3.6383.

[4] Kameyama A, Katto M, Yokotani, Atsushi. A Simplified Fabrication Technique for Tilted Fiber Bragg Gratingfor the Simultaneous Measurement of Refractive Index and Temperature of Liquids. *Journal of Laser Micro/Nanoengineering*. 2014; 9(3):230-233.

[5] Jiang B, Rauf A, Zhao J, Qin C, Jiang W. *Applications of Tilted Fiber Bragg Grating in Liquid Parameters Measurement*. Proceeding of SPIE 8788: Optical Measurement Systems for Industrial Inspection VIII. Munich. 2013: 878812. DOI: 10.1117/12.2019874.

[6] Yang HZ, Ali MM, Islam MR, Lim KS, Gunawardena DS, Ahmad H. Cladless few Mode fiber Grating Sensor for Simultaneous Refractive Index and Temperature Measurement. *Sensors and Actuators A: Physical*. 2015; 228: 62-68. DOI: 10.1016/j.sna.2015.03.001.

[7] Huang JY, Roosbroeck JV, Vlekken J, Martinez AB, Geernaert T, Berghmans F, Hoe BV, Lindner E, Caucheteur C. FBGs Written in Specialty Fiber for High Pressure/High Temperature Measurement. *Optics Express*. 2017; 25(15): 17936-17947. DOI: https://doi.org/10.1364/OE.25.017936.

[8] Li J, Zhang W, Gao S, Bai Z, Wang L, Liang H, Yan T. Simultaneous Force and Temperature Measurement Using S Fiber Taper in Fiber Bragg Grating. *IEEE Photonics Technology Letters*. 2014; 26(3): 309-312. DOI: 10.1109/LPT.2013.2293132.

[9] Amos, S, Prabu R, Njuguna P. *Theoretical Design and Analysis of a Sensing System for High Pressure and Temperature Measurement in Subsea Underwater Applications*. Proceeding of the 60th MTS/IEE Oceans conference (OCEANS'17), Aberdeen. 2017; Article ID: article ID 8085023. DOI: https://doi.org/10.1109/OCEANSE.2017.8085023.

[10] Xinhua Y, Mingjun W, Xiaomin C. Deformation Sensing of Colonoscope on FBGSensor Net. *TELKOMNIKA Telecommunication Computing Electronics and Control*. 2012; 10(8): 2253-2260.

[11] Bing W, Xiaoli W. Strain Transfer and Test Research of Stick-up FiberBragg Grating Sensors. *TELKOMNIKA Telecommunication Computing Electronics and Control*. 2014; 12(3): 589-596. DOI: 10.12928/TELKOMNIKA.v12i3.107.

[12] Bayuwati D, Waluyo TB. Macro-bending Loss of Single-mode Fiber Beyond Its Operating Wavelength. *TELKOMNIKA Telecommunication, Computing, Electronics and Control*. 2018; 16(1):142-150. DOI: 10.12928/TELKOMNIKA.v16i1.6666.

[13] MouniaC, Otman A, Badiaa AA, Fahd C, Vazquez AA, Mounir EY. Gain Flatness and Noise Figure Optimization of C-Band EDFA in 16-channels WDM System using FBG and GFF. *Journal of Electrical and Computer Engineering*. 2017; 7(1): 289-298. DOI: 10.11591/ijece.v7i1.pp289-298.

[14] De Sterke CM, Jackson KR, Robert BD. Nonlinier Coupled-Mode Equations on a Finite Interval: A Numerical Procedure. *Journal of the Optical Society of America B*. 1991; 8(2):403-412. DOI: 10.1364/JOSAB.8.000403.

[15] Ikhlef A, Hedara R, Chikh-Bled M. Uniform Fiber Bragg Grating Modelling and Simulation Used Matrix Transfer Method. *International Journal of Computer Science Issues*. 2012; 9(2): 368-374.